# Lunar Autonomous Scalable Emitter and Receiver (LASER) System
# NASA 2020 BIG Idea Challenge – Final Report


**Prepared By:**

Colorado School of Mines
1500 Illinois St.
Golden, CO 80401

CSM Team:
Ross Centers (Graduate, Space Resources)
Loren Kezer (Graduate, Space Resources)
Joshua Schertz (Graduate, Space Resources)
Curtis Purrington (Graduate, Space Resources)
Timofey Broslav (Graduate, Space Resources)
Adam Janikowski (Graduate, Space Resources)
John Schmit (Graduate, Space Resources)
Jef Hinton (Graduate, Space Resources)
David Dickson (Graduate, Space Resources)

UA Team:
Leonard Vance (Graduate, Aerospace E.)
Himangshu Kalita (Graduate, Aerospace E.)
Alvaro Diaz-Flores (Graduate, Aerospace E.)
Jose Fernandez (Graduate, Aerospace E.)
Jekan Thangavelautham (Advisor, Aerospace E.)

Faculty Advisor:
George Sowers
Email: gsowers@mines.edu
Phone: 303-384-2300

Space Grant Affiliation:
Colorado
Director: Chris Koehler
koehler@colorado.edu


**Prepared For:**

NASA BIG Idea Challenge
National Institute of Aerospace
1100 Exploration Way
Hampton, VA 23666

Date Submitted: 29 November 2020

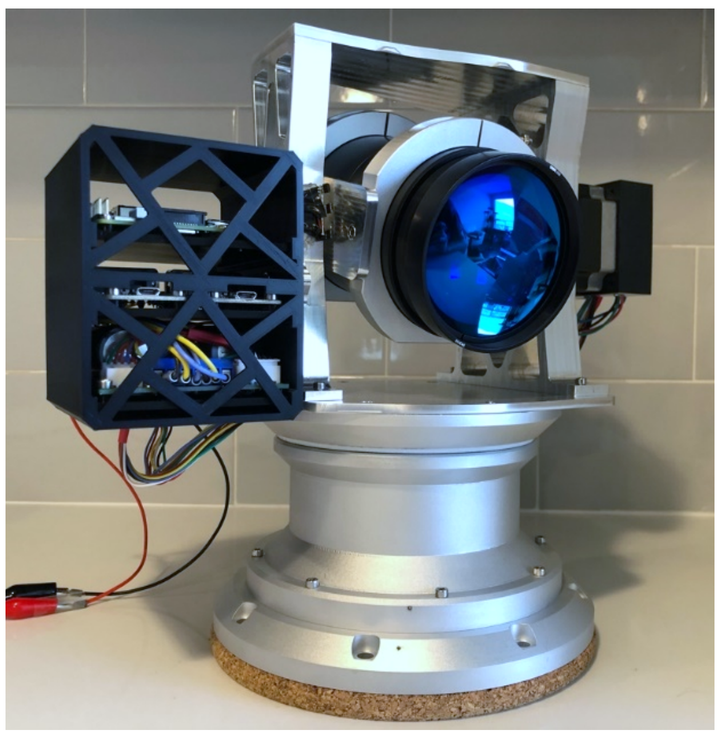

NASA COLORADO SCHOOL OF MINES THE UNIVERSITY OF ARIZONA BIG IDEA CHALLENGE

## Lunar Autonomous Scalable Emitter and Receiver (LASER) Team

COLORADO SCHOOL OF MINES


Ross Centers


Loren Kezer


Joshua Schertz


Curtis Purrington

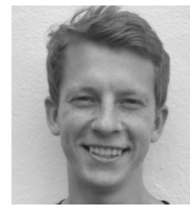
Timofey Broslav


Adam Janikowski


David Dickson


John Schmit


Jef Hinton


George Sowers


Leonard Vance


Himangshu Kalita


Alvaro Diaz-Flores


Jose Fernandez


Jekan Thanga

THE UNIVERSITY OF ARIZONA

# Colorado School of Mines Lunar Autonomous Scalable Emitter and Receiver (LASER) System

## CONCEPT SYNOPSIS

- A minimum viable demonstration of laser power beaming developed for a CLPS mission to the lunar surface.
- A lander-mounted laser transmitter autonomously identifies and charges stationary receivers ejected from the lander deck.
- Proof of concept to provide a scalable power delivery solution for systems in challenging space environments such as PSRs.

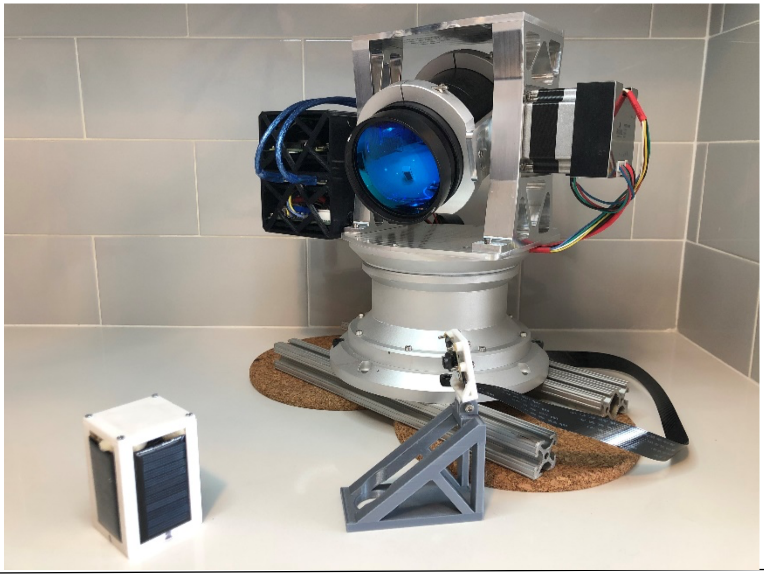

## INNOVATIONS

- A laser transmitter featuring 4W beam power at 793nm, 75mm collimating optics, with azimuth and elevation actuators and a beam control system.
- A FemtoSat based receiver, with solar arrays on four sides of the structure, which contains a computer, charge controller, battery, radio, and inertial measurement unit.
- Closed loop target detection and aiming for autonomous operations.
- Presented work at the 2020 International Astronautical Congress.

## PROOF-OF-CONCEPT TEST RESULTS & CONCLUSIONS

- Demonstrated laser power beaming at range of 30 meters.
- Demonstrated autonomous target detection and aiming.
- Tested FemtoSat survival during simulated lunar surface deployment.
- Concept should be scaled in power and range to enable rover operations in permanently shadowed regions.
- Submitted proposal “Laser Power Beaming for Remote and Mobile Applications” to NASA’s lunar surface technology research (LuSTR) program.

## 1. Table of Contents


Table of Figures ........ 2
Table of Tables ........ 3
Executive Summary ........ 1
1. Problem Statement and Background ........ 1
2. Project Description ........ 2
2.1. Concept Description ........ 2
2.1.1. Concept Lifecycle ........ 2
2.1.2. Design Decisions ........ 12
2.1.3. Design Changes Post Mid-Project Review ........ 13
2.2. Technical Specifications ........ 14
2.3. Integration with External Systems ........ 16
2.4. Science and Exploration Needs ........ 16
2.5. Stakeholders and Funders ........ 16
3. Proof-of-Concept Testing on Earth ........ 17
3.1. Verification Process ........ 17
3.2. Data Collected ........ 19
3.3. Challenges ........ 20
3.4. Testing Facilities ........ 20
3.5. Realistic Simulated Environment ........ 20
3.6. Budget and Schedule Constraints ........ 21
4. Safety Plan and Protocols Followed ........ 21
5. Path-To-Flight ........ 21
5.1. Lunar Mission ........ 21
5.2. Component Qualification ........ 22
5.3. Remaining Design Work ........ 22
5.4. Continuation of Concept Development ........ 22
6. Results/Conclusions ........ 23
6.1. Achievements of Objectives ........ 23
6.2. Key Results ........ 23
6.3. Conclusions about Design Solution ........ 23
7. Detailed Timeline ........ 24
8. Detailed Budget ........ 24
8.1. Phase 1 & Phase 2 Funding Awards ........ 24
8.2. Sponsors and Grants ........ 24
8.3. Outside Funding ........ 24
8.4. Sponsorships or in-kind contributions ........ 24

## Table of Figures

Figure 1: LASER System Architecture: Max Laser Output is 4W. ....2
Figure 2:CONOPS for the LASER System ....3
Figure 3: (A) The 4W Laser Diode Attached to the TEC Cooler. (B) The Fiber Connector after being Polished with 1-Micron Polishing Paper. ....4
Figure 4: (A) The First Iteration Optical Design Used a 50 mm Collimating Lens in an Open Optics Cage. (B) The Second Iteration Optical Design used a 75 mm Collimation Lens within an Optical Tube. The Beam Delivery Fiber is Visible in Yellow. ....4
Figure 5: The First Iteration Structure Enabled Testing of the Actuation and Control Logic. It Included a Lidar Unit and 5 mW Laser for Stepper Accuracy Tests. ....5
Figure 6: The Second (Left) and Third (Right) Structural Designs, called Affogato and Breve, Respectively. ....5
Figure 7: The FemtoSat Electronics Stack (Top) and the Wiring Diagram (Bottom). ....6
Figure 8: The LASER Software Architecture is Comprised of a Python API and React JS Web App, Enabling Full Control of the System Even When Testing in a Sealed Vacuum Chamber. ....7
Figure 9: A Custom Developed Front-End Client Acted as the Control GUI for the System, Enabling Full Status Monitoring and Control of the System. Shown is the Receiver Localization Process Locking onto the FemtoSat. ....8
Figure 10: Power Testing Apparatus (Left) and Power Curve (Right) - Input Power (Orange), Output Power (Gray), Efficiency (Yellow). ....8
Figure 11: Beam Image and Quantified Beam Profile. Beam Radius is 3cm. The Circumferential Intensity Peak is from Spherical Aberration of the Lens that is not Collimated but Aligns in the Limited Space of the Optics Lab. ....9
Figure 12: Receiver Bus Voltage (Blue) Responding to Sequential Solar Illumination of each PV Module (Purple, Yellow, Green, Red). Y Axis is Volts/100 for Bus Voltage, Unscaled for PV Response, X Axis is Time). ....10
Figure 13: A Simulation of the FemtoSat Receiver Being Ejected from the Lander’s Top Deck. The Transmitter is Visible on the Left. ....11
Figure 14: CAD (A) and Built (B) “Breve” Transmitter for Ground Demonstration. ....12
Figure 15: The FemtoSat Receiver Prototype Measures 3x3x6cm and has PV Modules on Four Sides. ....13
Figure 16: Schematic of the Breve Laser Transmitter, Detailing Dimensions, Parts & Materials, and Mass. ....14
Figure 17: Visualization and Schematic of the 4 W Laser used in the Transmitter ....15
Figure 18: Power Transfer over 30 Meters. Clockwise from Top Left: (A) The Illuminated FemtoSat Receiving Power, (B) The Optics Tube Transmitting Power Over 30m, (C & D) Configuration of the Experiment. ....17
Figure 19: Collimated Beam Width for a Fixed Focus at Ranges up to 30 Meters. Spot Size Showed Little Divergence. ....18
Figure 20: (A) Control (Left), LHS-1 (Middle), and JSC1-A (Right) Regolith Simulant on Photovoltaic Module. (B): The Effect of Regolith Simulant on Output Power. ....18
Figure 21: The Effect of a Partially Buried Receiver Panel on Output Power. ....19
Figure 22: FemtoSat Receiver after Simulated Ejection ....19
Figure 23: A Long-Range Laser Power Beaming System with Integrated Power Generation Sending Power to a Prospecting Rover Operating Unseen Deep within a PSR. ....22
Figure 24: A Prospecting Rover Operating Deep within a PSR Powered by a Laser Power Beaming Station Located High Above on the Sunlit Crater Rim. ....23

## Table of Tables

Table 1: Mission Objective and Top-Level Requirements. .......... 2
Table 2: Maximum Charging Efficiency with a MPPT Controller of 5.63% .......... 10
Table 3: Constraints of the BIG Idea Challenge .......... 14
Table 4: Laser Transmitter Power Budget .......... 15
Table 5: FemtoSat Power Budget .......... 15
Table 6: Team LASER's Schedule Over the Period of Performance .......... 24
Table 7: Executed Budget .......... 24

## Executive Summary

Our BIG Idea the "Lunar Autonomous Scalable Emitter and Receiver" (LASER) system, is a minimum viable demonstration of wireless power transmission for flight on a CLPS lander. Power transmission using lasers provides a scalable solution for delivering energy to systems in challenging space environments, particularly in and around lunar permanently shadowed regions (PSRs). The dramatic illumination and topography around the lunar poles encourages solutions that generate power in energy rich regions (peaks of high illumination) and move it to areas of high demand (such as PSRs) [Landis, Centers].

Our team developed and executed an integrated ground demonstration of the LASER concept, consisting of a laser transmitter powering ejectable remote receivers, linked by a telemetry system enabling closed loop aiming and beam control. We demonstrated laser power beaming over 30 meters, autonomous target detection and beam control, and tolerance of the receivers to dust and impacts. TRL advancement from 3 to 4 occurred through testing in a predominantly laboratory environment. Relevant environment testing under vacuum can advance TRL to 5 or 6. Due to COVID-19 related delays, vacuum testing has not yet been fully achieved, but we are prepared to do so when able.

The technology development approach was based on agile methodology while adhering to proven system engineering processes. Iterative subsystem designs provided quick feedback, while mitigating the impact of COVID-19 related supply chain issues and lab access limitations. Despite the extraordinary conditions of 2020, we were able to complete three revisions of transmitter design and two revisions of the receiver, culminating in the demonstration of laser power beaming over a distance of 30 meters and autonomous target localization.

In advancing the TRL of laser power beaming, we increased confidence in the feasibility of the concept, built an experienced team, and identified a technology maturation path for scaling up the concept to power rovers. With commercial and academic partners, we have responded to NASA's Lunar Surface Technology Research (LuSTR) solicitation with the proposal "Laser Power Beaming for Remote and Mobile Applications" to develop commercially relevant power beaming technology with a path to flight in by 2025.

## 1. Problem Statement and Background

The discovery of water ice in permanently shadowed craters at the Moon's poles [Colaprete; Li] is one of the most consequential findings of planetary science to date. Lunar water could be mined, purified, and electrolyzed into an extraterrestrial source of propellant: breaking the tyranny of the rocket equation, enabling exploration throughout the solar system, and catalyzing a cislunar industrial economy [CLPS; Kutter and Sowers]. Exposed water on the Moon, which is stable under vacuum only at temperatures below 100K, is found only in permanent darkness where energy is absent. To access this water, rovers need additional power sources beyond direct solar energy.

For example, in order to investigate polar volatiles, NASA's VIPER rover needs to operate in PSRs, but can only charge its batteries in sunlight. Consequently, the mission profile requires regular entry and exit from PSRs under battery power. The mission timetable must be choreographed to the availability of sunlight, where temporary delays risk mission loss due to battery depletion. Laser power beaming enables mission architectures that generate power in solar energy rich regions and move it to areas of high demand, such as PSRs. With a laser power beaming system, a lander on the rim of a large PSR could continually power a VIPER-like rover within line of sight by illuminating a rover mounted energy receiver with a power beam that tracks the vehicle. Such a system would allow a rover to stay in the PSR indefinitely.

Our concept is a minimum viable technology demonstrator for wireless energy transmission by laser power beaming (*Table 1*). The constraints of the BIG Idea Challenge offer an opportunity for creative mission design to fit a power beaming demonstrator in an 8W power budget (40W peak) and 15kg mass limit (which should be minimized with a $1M/kg cost of delivery to the lunar surface). By reducing risk, demonstrating feasibility, and increasing the TRL of this concept, our team's "Big Idea" will lead to increasingly capable iterations of laser power beaming technology to explore the Moon's discovered [Li] water resources within PSRs.

*Table 1: Mission Objective and Top-Level Requirements.*

| **Mission objective: Demonstrate laser power beaming on the lunar surface from a lander to a remote receiver, within 8W power and 15kg mass budget** |
|---|
| **Top level requirements:** |
| **- Eject a receiver 10m from the lander** |
| **- Autonomously locate the receiver and direct a laser power beam to illuminate it** |
| **- Charge the receiver's battery with the laser power beam** |
| **- Have multiple receivers for redundancy** |

## 2. Project Description

### 2.1. Concept Description

The LASER concept is an integrated architecture consisting of laser transmitter directing the collimated output of a fiber-terminated diode laser mounted on the top deck of a CLPS lander (*Figure 1*), and ejectable FemtoSat receivers developed by the University of Arizona's SpaceTREx Laboratory [Thangavelautham], contained within ejector pods oriented to deploy the receivers within the transmitter's field of view. The subsystems communicate via an RF network, with the transmitter autonomously locating each receiver and powering it with a laser beam. Multiple receivers are carried for redundancy in case of landing in an unfavorable orientation or behind occluding terrain. Telemetry is used to communicate charge status and enable closed-loop beam control.

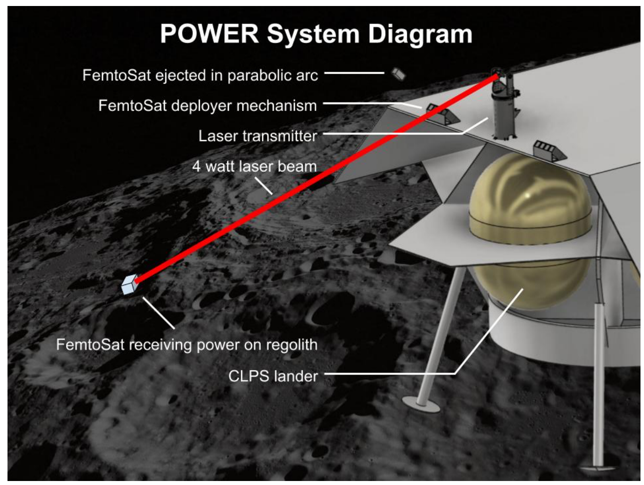


*Figure 1: LASER System Architecture: Max Laser Output is 4W.*

#### 2.1.1.1. Concept Lifecycle

The LASER ConOps is shown in *Figure 2*. The system is launched on a CLPS lander and delivered to the lunar surface. Upon landing, the system is activated and receivers deployed. Receiver landing locations are determined by raster scanning the laser over a search area defined by RF triangulation. When the laser illuminates a receiver's photovoltaic module, power telemetry indicates this to the transmitter. The system determines which receivers are most in need of power, and the transmitter illuminates the appropriate targets. Receivers send telemetry back to the transmitter throughout the mission duration.

The constraints of the BIG Idea Challenge motivated early concept studies that defined the high-level system architecture and defined top-level requirements. Upon project funding, the team began iterative development of the transmitter and receiver. As described in the development sections below, the optics design underwent two iterations, the transmitter had three iterations, and the receiver had two iterations.

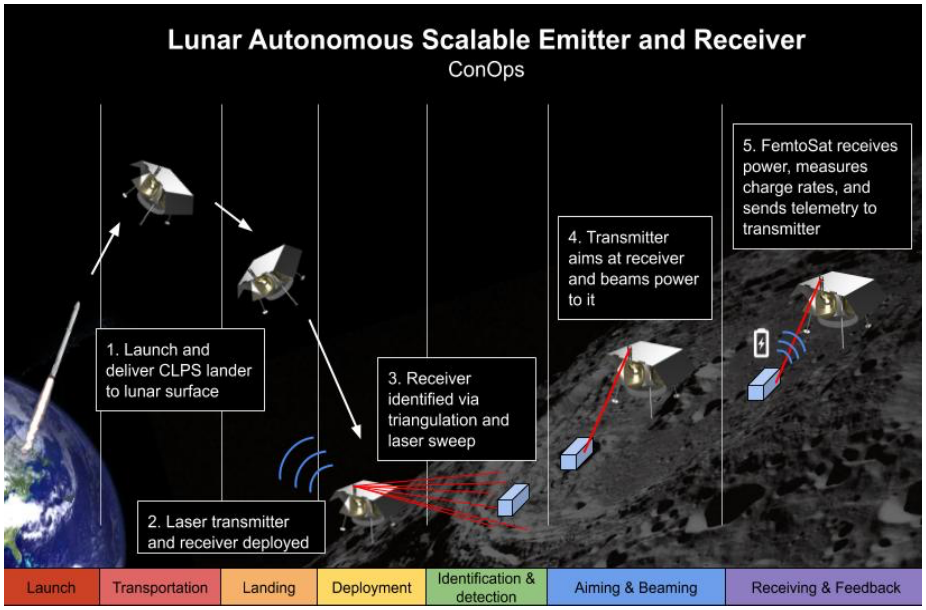


*Figure 2:CONOPS for the LASER System*

#### 2.1.1.2. Assumptions

Assumptions were made to enable rapid development. Prioritizing functional demonstration to increase TRL, we assumed that none of the selected components would be space qualified. Additionally, we assumed that risk reduction on low TRL technologies, such as the wireless power transfer link, would be more useful than validating incremental adaptations of high TRL technologies like spring-loaded ejectors.

Launch forces are assumed to be manageable as the system is based on solid-state technology and uses a robust structural design. We assumed the presence of an ejectable dust cover for landing, and that a flight power supply running off the 28VDC lander power at 8W-40W would be available. We assumed that our software could serve as a reference design for creating a flight-ready software control system on radiation-hardened computers or embedded microcontrollers.

Due to the illuminated landing site and the assurance of constant power, we assumed that cooling rather that heating would be the dominant thermal constraint of the transmitter. Its design features an integrated radiator surface that could be scaled for maximum effectiveness. We assumed that the mission profile would assure laser heating of receivers that land in shadow.

#### 2.1.1.3. Development

Initial development of our equipment fell into two main categories: hardware and software. Hardware was further broken down into the transmitter optics, transmitter structure, and FemtoSat receiver. Software development was broken into overall architecture and localization. In order to progress during COVID-related disruption, we focused on agile, iterative methods to maximize technology maturation of the system as resources and lab availability permitted.

**Hardware - Optics**

The choice of laser is central to the system architecture. Purchasing at the peak of COVID-related supply chain fears led us to choose a laser that was readily available and offered flexible mounting options. A 793nm diode laser, close to our desired 808nm specification, was available – a wavelength that would power any choice of photovoltaic module. The fiber-terminated package allowed rapid design iteration by largely decoupling laser mounting, power, and cooling requirements from transmitter design (*Figure 3*). We found that fiber beam delivery is architecturally attractive because it allows mounting the beam source separately from the optics, maximizing ease of cooling. Our architecture is designed with laser cooling in mind, but we used a benchtop laser diode driver and heat sink for development and demonstration. A miniaturized diode driver specific to the mission would need to be developed for flight.

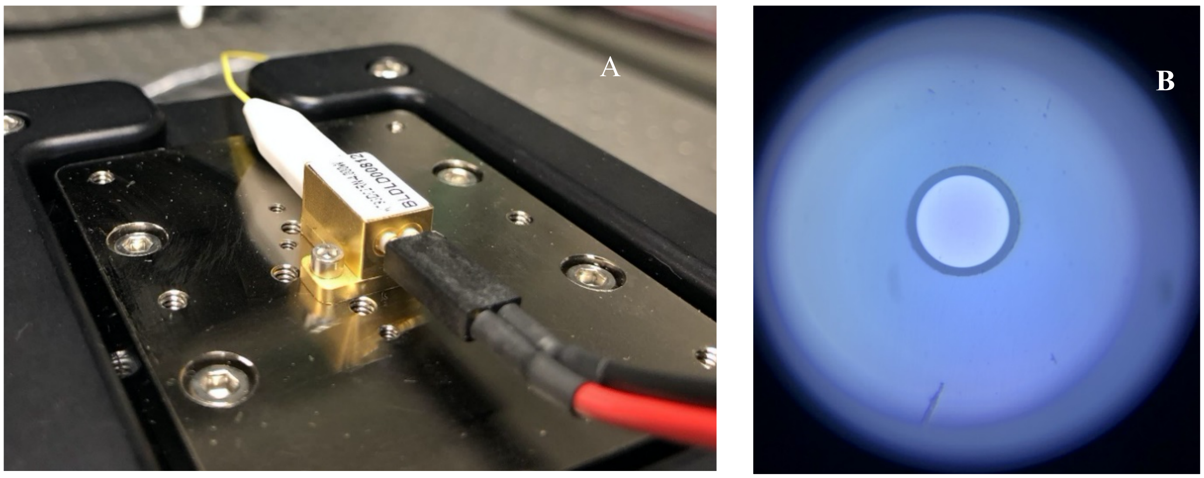


*Figure 3: (A) The 4W Laser Diode Attached to the TEC Cooler. (B) The Fiber Connector after being Polished with 1-Micron Polishing Paper.*

Because a raw fiber termination is burdensome to work with, we installed an FC/APC connector at the end of the fiber pigtail, providing secure mounting to the optics assembly. This required epoxying the fiber into the connector and polishing the connector tip to a 1-micron smoothness. Our initial design called for a 50mm collimating lens at 200mm focal distance, which we prototyped in an open optics cage, as seen in *Figure 4*. Based on results from testing, we iterated the design to use a 75mm collimating lens mounted within an aluminum optics tube with a focal length of 150mm. This second design better matched our laser diode's characteristics, while also enabling a larger spot size that was better suited for the elongated FemtoSat receiver (60mm on its long axis). Additionally, the enclosed optics tube provided direct integration into the transmitter structure.

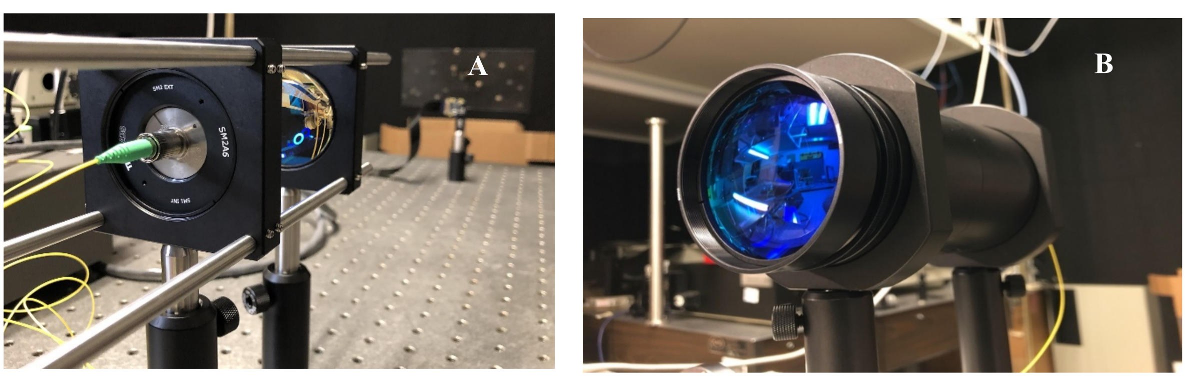


*Figure 4: (A) The First Iteration Optical Design Used a 50 mm Collimating Lens in an Open Optics Cage. (B) The Second Iteration Optical Design used a 75 mm Collimation Lens within an Optical Tube. The Beam Delivery Fiber is Visible in Yellow.*

**Hardware - Structure**

The transmitter structure went through three major iterations. The first iteration, shown in *Figure 5*, was a small unit that enabled early evaluation of actuation and control logic. This unit was 3D printed, used small stepper motors for azimuth and elevation joints, and was controlled via an Arduino MEGA. A 5mW laser pointer and lidar unit were attached to the structure, which were used to test pointing accuracy.

*Figure 5: The First Iteration Structure Enabled Testing of the Actuation and Control Logic. It Included a Lidar Unit and 5 mW Laser for Stepper Accuracy Tests.*

The second iteration unit was designed and built within the constraints of utilizing parts on hand during the initial COVID pandemic lockdown. The goal of this unit, named "Affogato" (*Figure 6*) after the espresso dessert, was to demonstrate integration of all components needed to run the laser transmitter. These components included azimuth and elevation steppers, a Raspberry Pi 3B+ computer, ancillary microcontrollers, and an optics mockup. The design featured a single compartment for all heat generating components to allow easier thermal management. Affogato was 3D printed and assembled at team member Josh Schertz's home, allowing concept development during lockdown.

With lessons learnt from the prior two iterations, work started on the third design, called "Breve" (*Figure 6*) after the espresso and half-and-half drink. Architectural goals for Breve focused on path-to-flight, machinability, structural support for the revised optics tube, and mounting for non-flight representative stepper motors. This final design was machined out of aluminum in the CSM machine shop. Aluminum was chosen as the structural material because it is easy to machine while allowing tight tolerances and robustness. PTFE bushings were used for the elevation and azimuth joints, providing smooth rotations without lubricant. Trinamic PAN-Drive stepper motors were chosen for the azimuth and elevation actuators, with the azimuth motor being stronger due to the increased mass it needed to rotate. Hall effect sensors were used to indicate the extreme rotation angles the elevation joint could rotate, ensuring the optics tube did not collide with the structure.

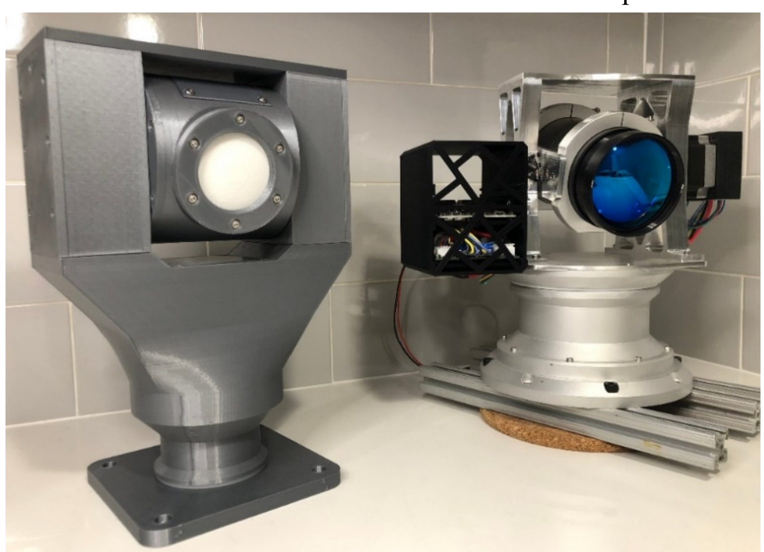

*Figure 6: The Second (Left) and Third (Right) Structural Designs, called Affogato and Breve, Respectively.*

All three designs used direct drive, which while easier to implement and fabricate, limited actuation accuracy and increased the actuator torque requirements. While stepper motors achieve peak torque above a few rpm, our design required operation below this threshold, limiting torque. Additionally, overcoming the stiction of the joints proved to be a challenge for small angle changes. A better design would use harmonic drives for both rotation joints that would provide much finer accuracy, smoother operation, and low backlash.

**Hardware – Receiver**

The FemtoSat receiver [Thangavelautham] was designed and built by teammates at the University of Arizona (UA) Space and Terrestrial Robotic Exploration Laboratory (SpaceTREx). It went through two iterations, with design objectives to measure 3x3x6cm, mass 80g, provide individual current measurement from each solar panel, and transmit telemetry over 433MHz radio link. The system utilized a TinyDuino microcontroller ["TinyDuino Overview"] that included an Arduino Pro Mini based microcontroller, USB interface, battery interface and charge controller, UHF radio, and breakout board. Four current sensors were used to measure each of the photovoltaic (PV) module's outputs. A 3.7V, 500mAh lithium-ion polymer battery was used to power the receiver, being charged by the PV modules. *Figure 7* shows the stack of TinyDuino boards that make up the FemtoSat, and the wiring diagram of all components within the stack. Due to the power draw of the analog current sensors used, a special chip was required to poll them at a reduced duty cycle.

Testing of the first integrated FemtoSat revealed current sensor magnetic interference. The second FemtoSat iteration used a similar component and wiring layout, but added MU-metal magnetic shielding for each current sensor. The second unit also included an IMU and environment sensor board that allowed the system to record impact forces, orientation, temperature, and pressure.

A TinyDuino based ground station interfaced between the FemtoSat and main Raspberry Pi computer. This unit only include a microcontroller, USB interface, and UHF radio.

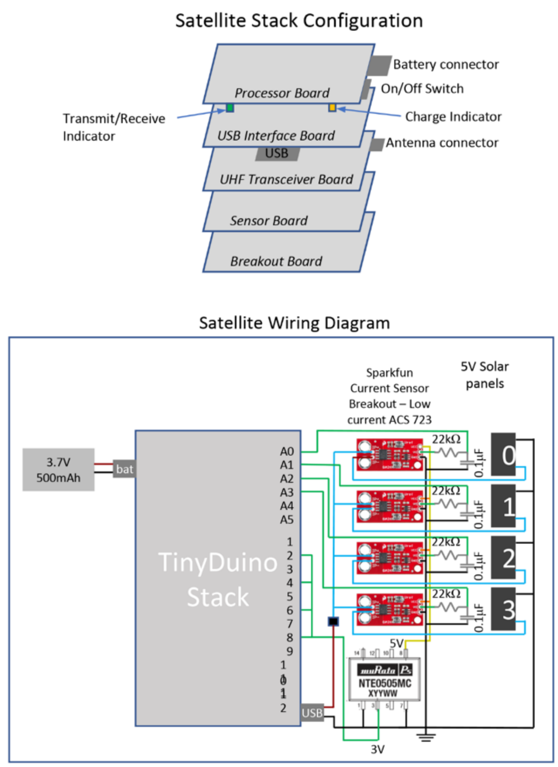


*Figure 7: The FemtoSat Electronics Stack (Top) and the Wiring Diagram (Bottom).*

**Software - Architecture**

The software architecture (*Figure 8*) was developed following software engineering practices of object-oriented programming (OOP), REST API design, and client-server design. The Raspberry Pi interfaces directly with both actuators, the ground station, and the WiFi access point. The developer can connect to the Raspberry Pi over WiFi to access the controller web app or the server directly via SSH. The web app acts as the control panel for the entire system, providing transmitter status, receiver status, control commands, and automated localization functions.

A Python Flask API provides the core logic for the system. It provides public API routes and threaded functions to interface with the actuators and ground station. Each Trinamic actuator is connected to the Raspberry Pi via a USB to CAN Bus interface. The actuators provide voltage, temperature, position, and load values, and can receive movement commands (based on either actual or relative positions). Hall effect sensors are connected directly to the elevation actuator, providing it rotation limit indicators and the ability to home itself to a central position. The ground station continually listens for telemetry signals from the FemtoSat receiver. The API is accessed via HTTP GET and POST commands from the front-end client.

The front-end client was built in React JS and acts as the control GUI for the system. It can be accessed via navigating a web browser to the Raspberry Pi's IP address on port 3000. As shown in *Figure 9*, the control panel displays system status, a live camera feed, manual movement commands, a graph of FemtoSat voltages, functions to connect, initialize, and shutdown the system, and the ability to start the automated raster scan. This interface dramatically improves the efficiency of integrated testing because the system can be controlled and monitored even when it's inside a sealed vacuum chamber.

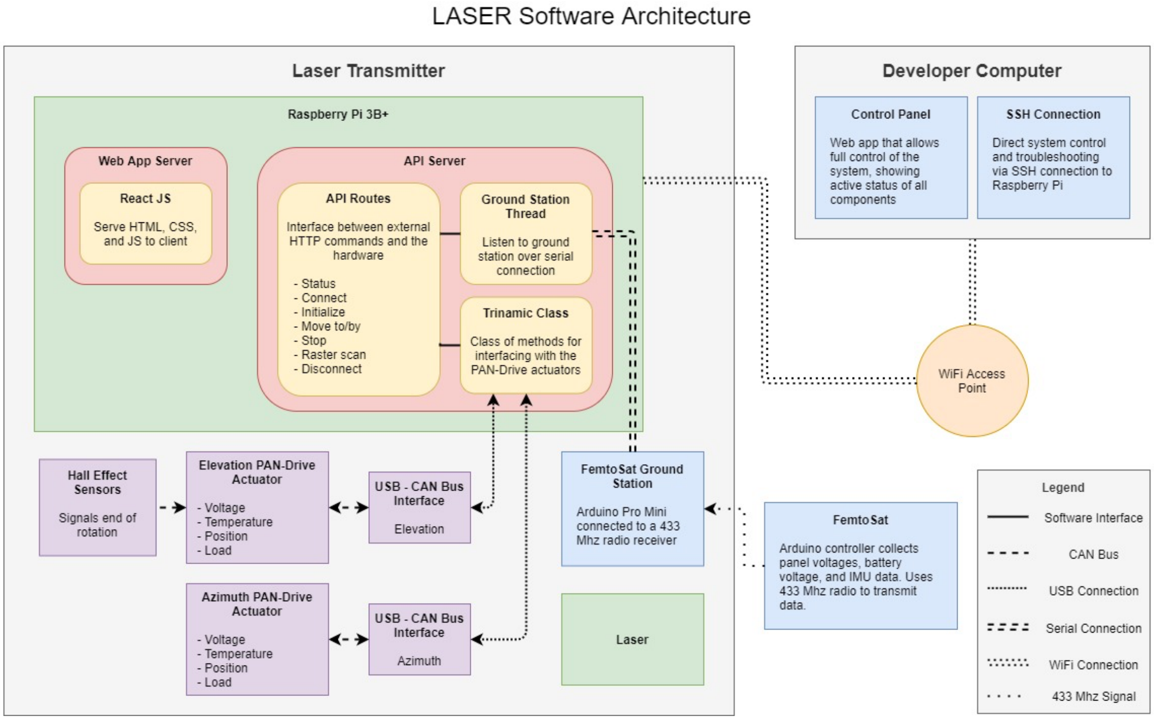


*Figure 8: The LASER Software Architecture is Comprised of a Python API and React JS Web App, Enabling Full Control of the System Even When Testing in a Sealed Vacuum Chamber.*

**Software - Localization**

The raster scanning logic was a state machine-based function that utilized closed loop feedback with the receiver over the RF telemetry link. The state machine flow is as follows:

1. Rotate the transmitter to the bottom left corner of the operation range
2. Rotate the azimuth to the right side of the range (default of 30 degrees)
3. Move the elevation up a small amount (default of 3 degrees)
4. Rotate the azimuth back to the left side of its scanning range
5. Repeat steps 2 to 4 until a current spike is detected from the receiver telemetry, indicating the beam fully illuminated the receiver (Figure 9); otherwise move to step 1.

The speed of the raster scan is based on the frequency of updates from the FemtoSat to the API. The current 1Hz ground station poll dictates a slow azimuth slew rate; otherwise, the laser would have slewed past the FemtoSat without having received the detection signal.

RF triangulation utilized Decawave DWM1001-DEV modules, which can provide real time 3D location data to 10cm accuracy using Time of Flight (ToF) via the 6.5GHz ultra-wideband (UWB) spectrum [Yavari and Nickerson]. When integrating these modules into our system, we placed three 'anchor' nodes with known positions around the transmitter and connected one 'gateway' node directly to the Raspberry Pi via its GPIO pins. The gateway node is the interface between the mesh network and the rest of the system. Lastly, 'tag' nodes were placed into mock-receivers that could be tracked across a large line of sight operating range. Proprietary algorithms within the Decawave modules calculated the location information. While the development modules used are too large for the UA FemtoSat, the core chip can be integrated directly on a custom PCB in future designs. Additionally, the system can scale to hundreds of tags, is able to facilitate data communications up to 6.8Mbps, and can operate at a very low power draw as shown in the interface in *Figure 9* [“DW1000 Radio IC”].

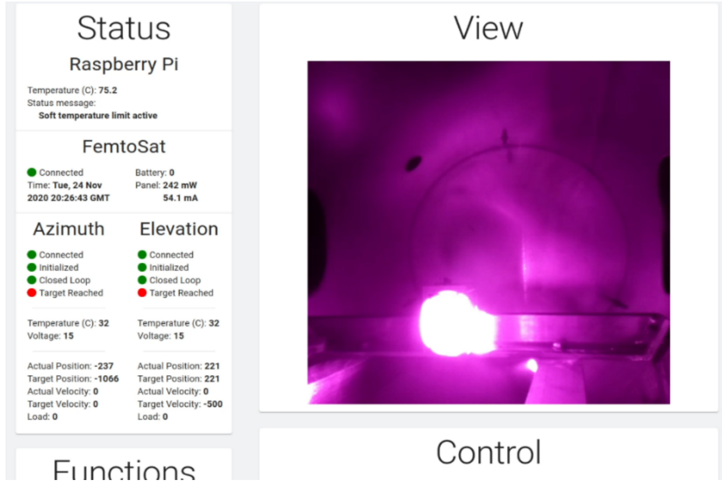


*Figure 9: A Custom Developed Front-End Client Acted as the Control GUI for the System, Enabling Full Status Monitoring and Control of the System. Shown is the Receiver Localization Process Locking onto the FemtoSat.*

#### 2.1.1.4. Testing

Testing of six individual components and subsystems was conducted before final integration.

**1.) Transmitter Laser and Optics**

Starting with the core of the system, the laser and beam were tested on an optical bench in a class 4 laser lab following procedures laid out in our laser safety plan. A Coherent PM150-50B thermopile sensor was used to measure total beam power (*Figure 10*). Lasing occurred at 1.7W input power, where an operationally useful 1.4W output beam was achieved at 4W input power. The laser reached its full rated beam power of 4.0W at 9.2W input power for a DC-optical efficiency of 43.6%.

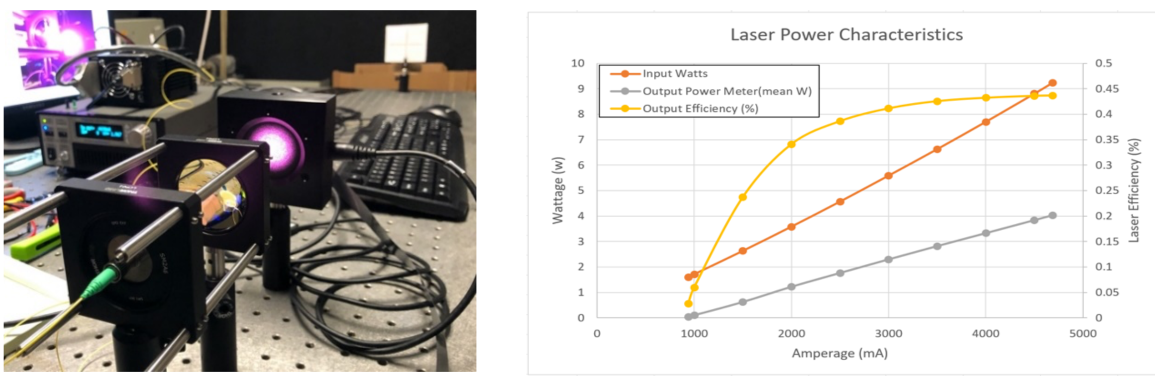


*Figure 10: Power Testing Apparatus (Left) and Power Curve (Right) - Input Power (Orange), Output Power (Gray), Efficiency (Yellow).*

The beam divergence at the fiber (prior to collimation) is important because it determines the spot size of the collimated beam in conjunction with the focal distance of the collimating lens. The manufacturer’s specification of a 0.22 numerical aperture (NA), or 12.7 degree beam width was represented to us as the full beam width, not the half beam width. Our initial design used a 50mm collimating lens with a focal length of 200mm, yielding a 44mm spot size at 0.22NA. However, after testing we realized that the full beam width was actually 0.44NA, or 25.2 degrees. Our optics design therefore required a redesign to accommodate this wider angle. The second iteration optical design utilized a 75mm collimating lens with a 150mm focal length, yielding a 66mm spot size. We installed the connectorized fiber and collimating lens into an enclosed optics tube with integrated fine focuser. The optics tube created a robust configuration that allowed the bench testing setup to be integrated into the final transmitter design (*Figure 10*).

Beam profiles using the final optics design were recorded in the laser lab. To profile the large 66mm spot size we used a Raspberry Pi No-IR camera (which did not include an IR filter) and 3D printed a fixture to align the camera with a laser test card. Custom software was written to adaptively adjust the dynamic range through multiple exposures, ensuring a perfectly exposed image was recorded. We flattened these beam images and processed them through another custom program to generate beam profiles, as shown in *Figure 11*. The collimating lens' spherical aberration generated a circumferential intensity peak at the limited ranges available in the optics lab (<=5 m), but the inner region of the beam indicates an approximately gaussian beam profile.

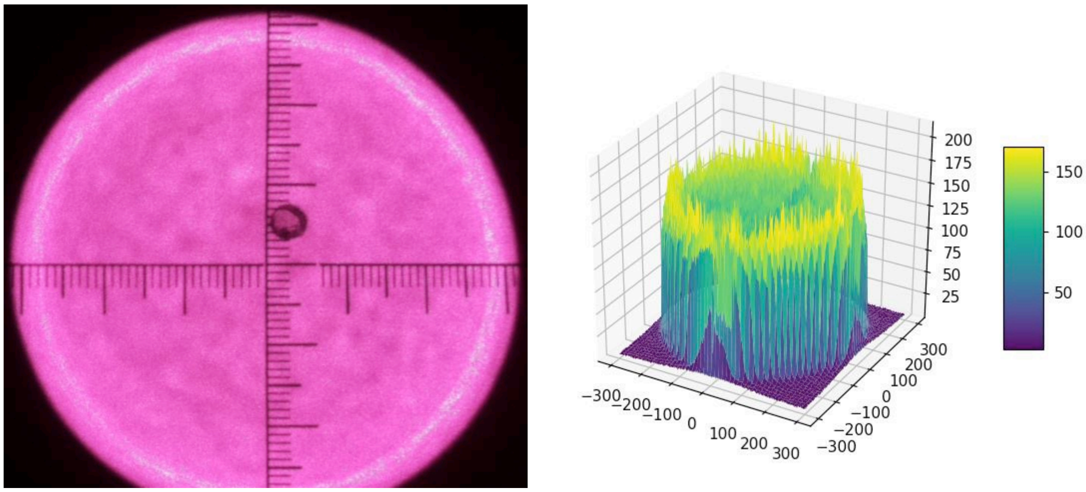


*Figure 11: Beam Image and Quantified Beam Profile. Beam Radius is 3cm. The Circumferential Intensity Peak is from Spherical Aberration of the Lens that is not Collimated but Aligns in the Limited Space of the Optics Lab.*

**2.) Transmitter Structure**

Testing of the transmitter structure focused on azimuth and elevation rotation accuracy. Although the stepper motors used for all design iterations are not flight hardware, we tested the hardware to understand how feasible our aiming requirement was. Starting with our first transmitter iteration, we tested the stepper accuracy at 3m range. Our results showed a reliable and repeatable accuracy of 0.56 degrees per step. While this does not meet the derived requirement of a 0.028 degree accuracy for aiming at 10m, it demonstrated that more powerful stepper motors utilizing micro stepping could achieve the requirement. This hypothesis was tested with our third and final design, Breve, using high performance Trinamic PAN-Drive stepper motors. Performing a similar accuracy test at 7.6m range, we demonstrated an average accuracy of 0.046 degrees for the azimuth and elevation axes. These accuracy results can be improved with joint refinement.

**3.) Receiver Detection and Aiming System**

Testing receiver detection and aiming was broken into three tasks, including tests of the telemetry link and state machine logic. The telemetry link flowed from the FemtoSat to the ground station to the Raspberry Pi and ultimately the API logic. Most pertinent was whether a FemtoSat panel was being illuminated by the transmitter's laser, and the frequency with which this data was transmitted to the Raspberry Pi. Tests showed that panel illumination was received and processed by the API within one second of illumination recording. This was based on a FemtoSat panel transmission at 2 Hz, and an API update status every second. More frequent updates would allow the transmitter to slew quicker during raster scans.

The raster scanning aiming logic was tested within Yakindu state machine software. This professional software allowed all permutations of the state machine logic to be evaluated, ensuring that each transition was valid. The state machine iterated between moving the azimuth to one limit of the search area, increasing the elevation slightly, then reversing the azimuth direction, monitoring for a FemtoSat panel current spike that would indicate illumination by the laser beam. This state machine logic was implemented within one of the API routes, which could be initialized by a command from the front-end client.

**4.) FemtoSat Receiver for Power Reception and Communication**

Tests included characterizing solar panels with a maximum power point tracking (MPPT) test, testing how the FemtoSat panels respond to light, and testing the current sensors. While the FemtoSat receiver was too small to house a MPPT charge controller, we wanted to test the maximum efficiency possible from our laser with a commodity silicon solar panel. We determined the maximum power point by using a 0-100ohm rheostat to vary the load across the panel, finding a maximum end-to-end energy efficiency (DC to DC) of 5.63%, as shown in *Table 2*. This includes geometric losses, as there is substantial beam spillover on the photovoltaic module.

*Table 2: Maximum Charging Efficiency of 5.63% via a MPPT test.*

| Voltage (V) | Current (mA) | Power (W) | Efficiency | |
|---|---|---|---|---|
| 0.275 | 155 | 0.04262500000 | 0.47% | |
| 2.8 | 153 | 0.42840000000 | 4.76% | |
| 2.9 | 152 | 0.44080000000 | 4.90% | |
| 3.8 | 113 | 0.42940000000 | 4.77% | |
| 3.1 | 152 | 0.47120000000 | 5.24% | |
| 3.3 | 151.5 | 0.49995000000 | 5.56% | |
| 3.4 | 148 | 0.50320000000 | 5.59% | |
| 3.6 | 129 | 0.46440000000 | 5.16% | |
| 3.45 | 145 | 0.50025000000 | 5.56% | |
| 3.42 | 148 | 0.50616000000 | 5.63% | R=26 ohm |
| 3.45 | 145.7 | 0.50266500000 | 5.59% | |
| 3.43 | 146.7 | 0.50318100000 | 5.59% | |

The FemtoSat's response to light across each of the unit's panels was tested. Each photovoltaic module was wired to an individual current sensor. As bright light was shone on each panel, the current sensor value associated with that panel spiked, indicating it was illuminated (*Figure 12*: Receiver Bus Voltage (Blue) Responding to Sequential Solar Illumination of each PV Module (Purple, Yellow, Green, Red). Y Axis is Volts/100 for Bus Voltage, Unscaled for PV Response, X Axis is Time).

During early testing of the FemtoSat under laser illumination, interference between current sensors was seen. The raw data showed that if panel 1 was illuminated, panel 3 on the opposite side of the unit would show a sharp negative value. Each panel showed different amounts of interference. This interference was caused by magnetic interference between current sensors and adjacent wiring of neighboring panels. The solution was to wrap MU-Metal foil around each current sensor to act as a magnetic field barrier. The second iteration FemtoSat included MU-Metal that improved the stability of the current sensor values. Packaging constraints dictated analog current sensors; digital current sensors could provide further improvements to the current sensing capabilities.

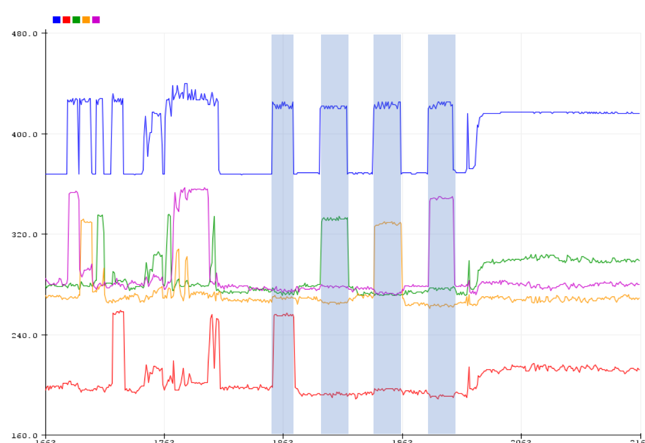


*Figure 12: Receiver Bus Voltage (Blue) Responding to Sequential Solar Illumination of each PV Module (Purple, Yellow, Green, Red). Y Axis is Volts/100 for Bus Voltage, Unscaled for PV*

**5.) Receiver Deployment Mechanism**

Simulation of the deployment mechanism was performed. The general concept is similar to traditional P-Pod deployers that are used for ejecting CubeSats [Puig-Suari]. These designs have extensive flight heritage and use a simple spring and burn-wire based mechanism. Simulation of the deployment was performed in Blender, where a model was tested using lunar physics. *Figure 13* shows a still frame from this simulation.


*Figure 13: A Simulation of the FemtoSat Receiver Being Ejected from the Lander's Top Deck. The Transmitter is Visible on the Left.*

**6.) Configuration of University Vacuum Chamber**

This project was the first time a high-power laser was operated within one of our lab's vacuum chambers. We utilized a medium sized cryovac chamber that is a horizontal cylinder with 1m internal length and 45cm diameter opening. We installed a fiber feed-through, laser safety interlock, and laser light blocking foil over both chamber windows. The fiber feed-through allowed the laser and support electronics to remain outside the chamber, while the fiber could be fed into the chamber. This kept the free-space beam path safely within the vacuum chamber. A 3mm hole was drilled into a blank vacuum plate, allowing the fiber to be fed through the hole and sealed with vacuum rated epoxy. After curing the required time, the plate was installed onto the chamber and tested for proper seal. A vacuum of 0.5tor was achieved with no discernable leaks detected. By enclosing the laser's fiber free-space interface within the sealed chamber with interlock, we ensured a class-4 laser could be operated as a class-1 laser, meeting the requirements of our safety plan.

#### 2.1.1.5. Implementation

Based on our original goals, we succeeded to varying degrees with the implementation of each:

1. **Deployment** – The first objective focused on safe stowage, initialization, and deployment. The final transmitter design, Breve, included a solenoid lock for the elevation axis. Dust covers, FemtoSat receiver stowage, and transport trickle charging were not evaluated. Analysis was performed on the forces required to deploy the FemtoSats in the lunar environment, including the impact forces experienced by each FemtoSat upon landing. The FemtoSat telemetry data acquisition upon deployment was implemented within the overall system software architecture, providing a robust mechanism for the receivers to inform the system of their status.
2. **Identification and Detection –** The identification and detection task was partially completed. The raster scanning process of finding a FemtoSat receiver using the main laser beam was fully verified. However, the time-of-flight localization was not integrated into the FemtoSat due to size constraints. We did acquire demonstration boards for RF mesh localization, but these have only been partially tested.
3. **Aiming** – Autonomous aiming was demonstrated. Fine aiming control was implemented for both axes with a precision of 0.046 degrees. The actuators used provide absolute positioning, while hall effect sensors on the elevation axis restrict movement to within a safe operation range. PTFE bushings were utilized instead of ball bearings because PTFE bushings have a much better operational thermal range, aided by their ability to run dry (without lubrication). A custom rotation mechanism was developed for the azimuth joint, using two PTFE thrust bushings and a POM radial bushing, providing a very robust mechanism. Aiming control was integrated into the API routes, allowing control of the system through the control panel and automated raster scanning logic.

4. **Power Beaming** – Power beaming was demonstrated to the FemtoSat receiver at ranges up to 30m. A bare panel efficiency test showed up to 5.6% DC-DC efficiency. The FemtoSat was able to charge at a laser output power of 1.4w. The final optical design was much simpler than the initial proposed design, using only a collimating lens within a rotating optical tube, instead of a separate beam director.
5. **Receiving** – The FemtoSat receiver was designed and built by SpaceTREx with commercially off the shelf (COTS) components, including four solar panels, a microcontroller with integrated charge controller, battery, and IMU. We demonstrated FemtoSat battery charging using the laser at ranges up to 30m. Various panel angles in relation to the laser were tested. FemtoSat status was able to be transmitted to the receiving ground station. Environmental impacts on the unit only focused on lunar regolith simulant accumulation, where no discernable effects were identified. Thermal and radiation interference were not addressed.
6. **Feedback** – We demonstrated that the FemtoSat can transmit charge rates, sensor readings, and IMU measurements across a 433MHz radio link to the transmitter at 2Hz poll rate. The low data rate was effective enough for raster scanning localization. However, multiple receivers operating in parallel would require a revised radio link method for the system to discern one receiver from another.

### 2.1.2. Design Decisions

#### 2.1.2.1. Transmitter

The transmitter (*Figure 14*) is an altitude/azimuth gimbal design built around an optical tube that supports a fiber terminated diode laser package delivering up to 4W beam power. The fiber emits the beam into free space in an enclosed optics tube, where it illuminates a 75mm collimating lens at the final aperture. The beam diameter is sufficient to completely illuminate the receiver while minimizing divergence at range.

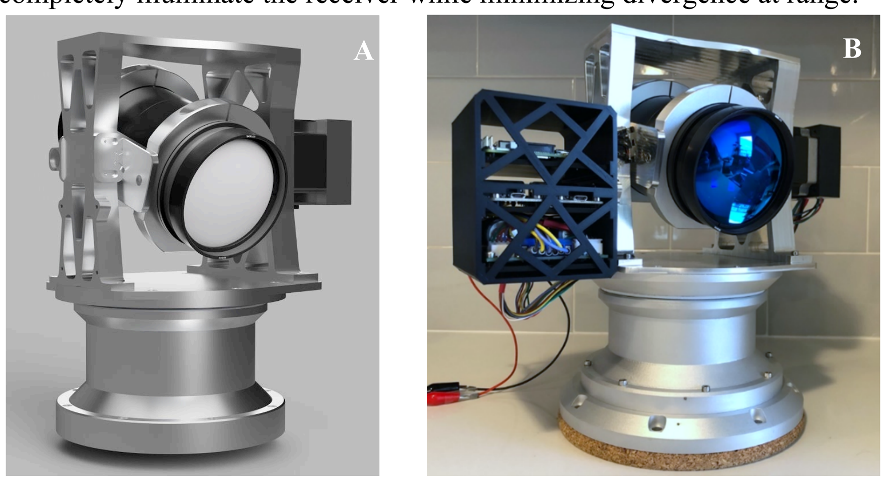


*Figure 14: CAD (A) and Built (B) "Breve" Transmitter for Ground Demonstration.*

The laser diode is mounted away from the optics tube, enabling better thermal management. Other heat generating components are attached to the main rotating structure, creating a fixed geometry of heat sources in relation to a horizontal radiator plate located at the very top of the structure. At the lunar poles, a horizontal radiator would provide an unobstructed view of space, creating a highly effective radiative surface – an ejectable dust cover would be required to protect it during landing. Further design work would thermally integrate these heat sources with the radiator.

The transmitter structure is constructed out of machined aluminum. It consists of 15 components fastened together with bolts. The azimuth joint uses an SKF POM composite bearing and two custom made PTFE thrust bushings. The elevation joint uses PTFE radial and thrust bushings for each side. In combination, these radial joints provide structural support for all orientations, increasing structural survivability.

Two Trinamic PAN-drive stepper actuators provide azimuth and elevation movement. A PD57-2-1378 is used for the azimuth actuator, and a PD57-1-1378 is used for the elevation actuator. The azimuth actuator is secured within the azimuth rotation joint, whereas the elevation actuator is mounted on the exterior of one of the optics support struts. Both actuators used direct drive that enabled a simple mechanical structure and minimal backlash at the expense of angular resolution, torque and mass. Microstepping is utilized to increase angular resolution, but this reduces torque. On flight hardware, zero backlash harmonic drives with integrated clutches would offer sub-milliradian pointing accuracy and zero-power holding. Improved harmonic drives could offer useful range limited only by beam quality and line of sight; we propose further design evolution in sections 5 and 6.

The transmitter uses a Raspberry Pi 3B+ running Raspbian Linux as its central computer. While the Raspberry Pi is not radiation hardened, the core code could be integrated into a hardened computer with heritage. Command and control of this system is handled via front-end client between a developer computer and the Raspberry Pi over a WiFi connection. Communication between the Raspberry Pi and actuators is handled over CAN Bus, allowing actuator variables to change in real time. The FemtoSat telemetry is received by a dedicated Arduino based ground station that is connected to the Raspberry Pi via a serial connection.

#### 2.1.2.2. Receiver

The receiver is optimized for simplicity and minimal mass. These design choices make it possible to rely on redundancy rather than high reliability for a lunar demonstration. The FemtoSat units (*Figure 15*) were developed and built by SpaceTREx, and measure 3x3x6cm with mass less than 80g. The design integrated solar cells and current sensors on four of the long faces, along with small battery, charge controller, radio, and microcontroller. With solar cells on multiple faces of the cube, the receiver can be charged in nearly all orientations, simplifying deployment.

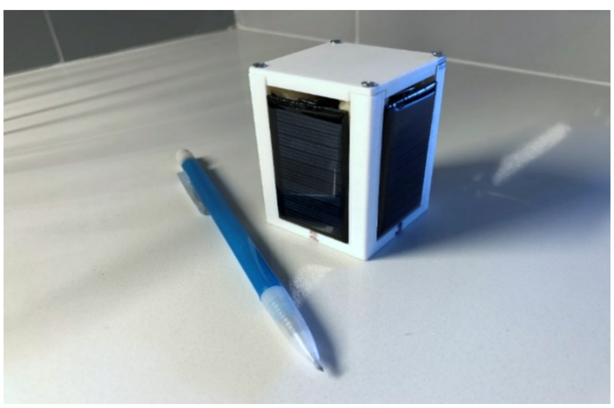

*Figure 15: The FemtoSat Receiver Prototype Measures 3x3x6cm and has PV Modules on Four Sides.*

In the early design phase, it became apparent that off-the-shelf charge controllers capable of working with the low voltages from a single cell were unavailable within the volume constraints. 3x6cm commodity silicon PV modules with 10 cells wired in series were used, with each module providing 3-5V output. The original design called for a 3x3x3cm receiver, but the constraints required the use of a slightly larger 3x3x6cm unit. This made it possible to stack the microcontroller alongside the battery and current sensors for each of the four solar modules, and to integrate an IMU and thermal sensors. The mass remains low at 80g.

### 2.1.3. Design Changes Post Mid-Project Review

A few minor design changes were made post mid-project review. After discovering that our laser's beam divergence at the fiber was twice the angle anticipated, we redesigned the optics path to feature a larger collimating lens at a closer focus. This shortened beamline allowed us to simplify the optics path, and the larger final aperture allowed better illumination of the FemtoSat receiver.

With space inside the FemtoSat receiver at a premium, we were unable to integrate RF localization into the design. Instead, we separately procured Decawave localization development boards to allowing the creation of a mesh localization network. These provide localization accuracies up to 10cm using RF time of flight. The actual chips (detached from the development PCB) could be integrated into a FemtoSat with additional engineering effort.

## 2.2. Technical Specifications

The technical constraints of the challenge are presented in *Table 3*. Except for total power and radiation tolerance, our solution meets the requirements. Power required will meet requirements with the substitution of the non-flight representative stepper motors for geared harmonic drive units with holding clutches. Our computer hardware is unlikely to survive the deep-space radiation environment, but software could be reimplemented on heritage radiation-hardened units.

*Table 3: Constraints of the BIG Idea Challenge*

| Initial Constraints |
|---|
| **Surface Mass** – Teams should start with a 15kg total packaged mass limit (including all mechanical and electrical components), unless there is a compelling reason that justifies additional mass. |
| **Power** - At least 8W continuous and 40W peak for 5 minutes |
| **Power Conditioning** - Regulated and switched 28Vdc |
| **Bandwidth** (i.e., rate which data can be sent to the lander) - At least 70kbps per kg of payload (if more is needed, internally store/buffer to stay under 70kbps) |
| **RF comm** (i.e., rate that can comm can be relayed to Earth) - 70kbps per kg max (if more is needed, internally store/buffer to stay under 70 kbps) |
| **Radiation** - 1krad max |
| **Wired Communication** - serial RS-422 |
| **Wireless Communication** - 2.4GHz IEEE 802.11n compliant WiFi |
| **Thermal Design** - should assume adiabatic mounting |

*Figure 16* shows the schematic of our Breve revision laser transmitter, which dominates the mass of our solution at 6.1kg. The Trinamic stepper motors are not flight-representative, nor are the compute modules. Their locations, however, are representative of a flight configuration.

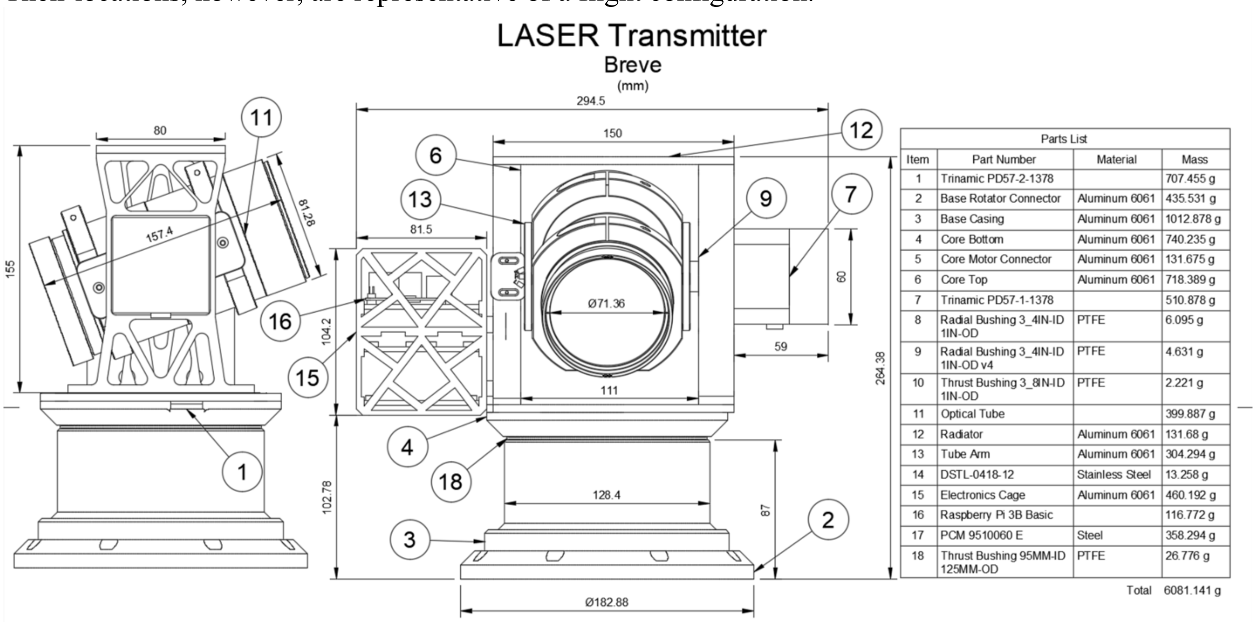


| Parts List | | | |
|---|---|---|---|
| Item | Part Number | Material | Mass |
| 1 | Trinamic PD57-2-1378 | | 707.455 g |
| 2 | Base Rotator Connector | Aluminum 6061 | 435.531 g |
| 3 | Base Casing | Aluminum 6061 | 1012.878 g |
| 4 | Core Bottom | Aluminum 6061 | 740.235 g |
| 5 | Core Motor Connector | Aluminum 6061 | 131.675 g |
| 6 | Core Top | Aluminum 6061 | 718.389 g |
| 7 | Trinamic PD57-1-1378 | | 510.878 g |
| 8 | Radial Bushing 3_4IN-ID 1IN-OD | PTFE | 6.095 g |
| 9 | Radial Bushing 3_4IN-ID 1IN-OD v4 | PTFE | 4.631 g |
| 10 | Thrust Bushing 3_8IN-ID 1IN-OD | PTFE | 2.221 g |
| 11 | Optical Tube | | 399.887 g |
| 12 | Radiator | Aluminum 6061 | 131.68 g |
| 13 | Tube Arm | Aluminum 6061 | 304.294 g |
| 14 | DSTL-0418-12 | Stainless Steel | 13.258 g |
| 15 | Electronics Cage | Aluminum 6061 | 460.192 g |
| 16 | Raspberry Pi 3B Basic | | 116.772 g |
| 17 | PCM 9510060 E | Steel | 358.294 g |
| 18 | Thrust Bushing 95MM-ID 125MM-OD | PTFE | 26.776 g |
| | | Total | 6081.141 g |

*Figure 16: Schematic of the Breve Laser Transmitter, Detailing Dimensions, Parts & Materials, and Mass.*

*Table 4* presents the power budget for our transmitter. While power beaming is inherently energy intensive, our non-flight representative stepper motors are the dominant power load. Flight hardware would consist of harmonic drive motors with clutches to hold position without power draw. The laser power can be throttled down to 1.4W beam power, or 3.25W DC, and still be able to power the receivers according to our testing.

*Table 4: Laser Transmitter Power Budget*

| ***Component*** | **Min Power (W)** | **Max Power (W)** | **Notes** |
|---|---|---|---|
| *Azimuth Actuator* | 3 | 15 | Very brief power peaks of 15W; average draw of 9W when moving; 3 W when stopped |
| *Altitude* Actuator | 3 | 14 | Very brief power peaks of 14W; average draw of 9W when moving; 3W when stopped |
| *Laser* | 3 | 9 | 3W is lowest power to charge receiver battery. 9W is max rated power. |
| *Control* Electronics | 4 | 4 | Raspberry Pi 3B+, Arduino Pro Mini, miscellaneous electronics |
| *Total* | 13 | 42 | More efficient flight actuators would allow system to fit within 8W steady state / 40W peak power envelope. |

We used a BWT 793nm 4W fiber coupled diode laser, model number K793D02RN-4.000W, as shown in *Figure 17*. The diode package is small, and the fiber allows mounting in a thermally favorable location.

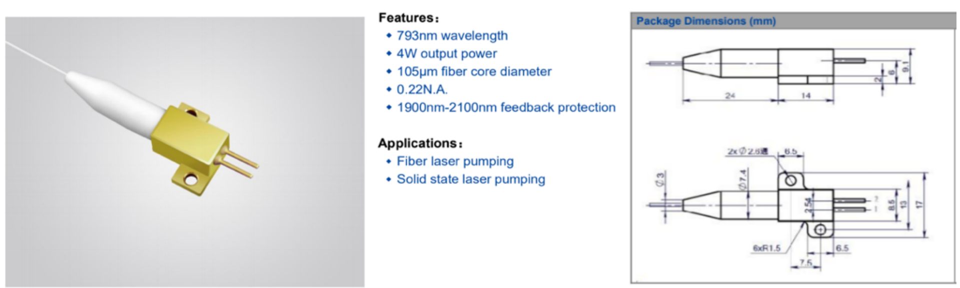


*Figure 17: Visualization and Schematic of the 4 W Laser used in the Transmitter*

The power budget for the receiver (*Table* 5) is derived from integrated battery, kept charged by PV modules illuminated by the laser. The microcontroller and sensors are all able to operate even with the battery charging. The battery is also able to remain powered on with no laser input for up to 90 minutes.

*Table 5: FemtoSat Power Budget*

| item | current (mA) | duty cycle | pro-rated current (mA) | Notes |
|---|---|---|---|---|
| processor board | 1.2 | 1 | 1.2 | specified by datasheet |
| USB interface board | 0 | 1 | 0 | unknown - unspecified |
| Comm board TX | 85 | 0.005 | 0.43 | 20dbm setting= 85 mA, 13dbm=30mA |
| Comm board RX | 18.5 | 0 | 0 | no receiver usage currently |
| Combo Sensor Board | 4.4 | 1 | 5.1 | |
| Current Sensor (5V) (each) | 9 | | | |
| NTE0305 Efficiency | 0.78 | | | |
| Current Sensor (3V) (each) | 19.2 | | | |
| Current Sensors total (3V) | 76.9 | 0.0833333 | 6.41 | 50 ms on, 550 off duty cycle |
| | | | | |
| total average current drain | | | 13.14 | mA (3-4 mA measured) |
| | | | | |
| Solar panel at 1kW/m2 | 20 | 1 | 20 | Measured midday Tucson |
| net solar level charge | | | 6.9 | mA |
| | | | | |
| Battery Capacity | 500 | mAh | | Specified battery capacity |
| Operating time | 19.0 | hours | | Assume 50% discharge depth |
| Charging time, S | 36.4 | hours | | from 50% discharge, assuming 1kW/m2 |

### 2.3. Integration with External Systems

The LASER system is designed to integrate with any CLPS lander. Flight hardware could interface with the lander power supply. The heat generating components of the transmitter are located in thermal contact with a top-mounted radiator that would have a continuous dark sky view at the lunar poles and can be scaled to provide the cooling necessary for adiabatic mounting. As an autonomous system, bandwidth requirements to Earth are minimal, and telemetry between the receiver and transmitter can fit within the 70kbps data budget. The transmitter and the receiver ejector can be mounted in a wide range of locations on the top deck, minimizing concerns of lander center of gravity or obstructions.

### 2.4. Science and Exploration Needs

The laser beam itself can be used to perform science objectives, such as heating regolith for other remote sensors to detect evolved volatiles. The FemtoSat receivers and the laser beam itself can be used to support science and exploration objectives. Each receiver contains an IMU and can capture geotechnical data upon impact with the regolith. The radio localization features integrated into flight hardware could serve as position beacons in establishing a navigational reference system.

Our concept also reduces risk toward deploying scaled up laser power beaming systems for rovers operating in PSRs, systems which could conduct game-changing science and exploration. NASA's Lunar Surface Technology Research (LuSTR) solicitation identifies a need for 100W of electrical power to be transferred to mobile rovers over 1km away from the transmitter, which would enable sustained exploration deep into PSRs. In response, our team has submitted a proposal "Laser Power Beaming for Remote and Mobile Applications" to achieve these objectives.

### 2.5. Stakeholders and Funders

Technology development for lunar power transmission is at an early stage, but the magnitude of the opportunity is increasingly well-recognized. We believe that the technology maturation path is one of early government support, with a transition to public-private partnership followed by maturation through commercial application. The BIG Idea Challenge provided an early opportunity to demonstrate the feasibility of laser power beaming for CLPS landers. During the course of our development, we have developed relationships with commercial partners Lockheed Martin, Roccor, Astrobotic, and PowerLight Technologies, collaborations with NREL, Naval Research Laboratory (NRL), and MIT's Haystack Laboratory, and identified further directions for partnership between CSM and UA.

With faculty advisor George Sowers as PI, our LuSTR proposal brings this team together to develop a mission architecture and ground demonstration for powering a VIPER-like rover several kilometers away from a lander-mounted power beaming station. Demonstrating power transmission of over 100W at greater than 2km, our team is prepared to demonstrate feasibility of unlimited-duration operations in PSRs and support a critical NASA exploration need. If funded, our university & commercial team would conduct this technology advancement in the 2021-2023 period of performance. During this period, a candidate flight mission will be developed, and the commercial capabilities established to fly a successor to VIPER with laser power beaming in the 2025-2026 timeframe.

Ultimately, laser power beaming is a key steppingstone on the path to developing a commercially viable extraterrestrial source of propellant, breaking the tyranny of the rocket equation and supporting exploration and human expansion throughout the solar system. NASA's support of prospecting missions at the lunar poles could create the scientific and technical confidence necessary to reach an ignition point after which commercial prospecting and public-private resource development could occur. Our research and partnerships build toward this desired outcome.

## 3. Proof-of-Concept Testing on Earth

### 3.1. Verification Process

This technology advancement iteration has reduced risk for laser power beaming by demonstrating feasibility of the underlying technology. The team developed a representative laser power beaming prototype that goes beyond an ad-hoc, "breadboard" type system. A purpose of the project was to test the system in an environment relevant to its intended lunar destination, especially regarding its performance with respect to dust, vacuum, and thermal considerations, advancing the system to TRL6. Due to COVID-related laboratory disruptions, we have to-date been unable to conduct a prototype demonstration in this relevant environment – accordingly, the system is currently at TRL4.

Design, fabrication, assembly, and preliminary testing was performed for the "Breve" prototype laser power beaming system at Colorado School of Mines, with power transmission and reception demonstrated over a long distance. To further advance the TRL, testing of the system in a relevant environment is required. Due to the COVID-19 pandemic, test plans using the lab's vacuum chamber have been postponed, but the team plans to conduct system level relevant environment testing before the end of the performance period in early January 2021. This testing can advance the system to TRL6.

The following verification demonstration and tests were performed: power beaming over a 30m distance, autonomous aiming and beam control, verification of power transfer through a dusty panel, demonstration of receiver survival during deployment onto a simulated lunar surface, and verifying operation in some lunar environmental conditions. The next subsections describe each of these demonstration/tests in turn.

**Power Beaming Demonstration over 30m**

Power beaming was verified up to 30m. While the laser lab only had a working distance of 5m, we sought out a location with a long span that followed laser safety requirements. Ultimately, an underground steam tunnel on campus was identified. The longest stretch of the tunnel was 30 meters, over which we were able to demonstrate charging the battery of the FemtoSat with laser power (*Figure 1*). End-to-end efficiency was recorded across the 30m distance, although this only used a static resistive load and not a MPPT charge controller that would provide optimal efficiencies.

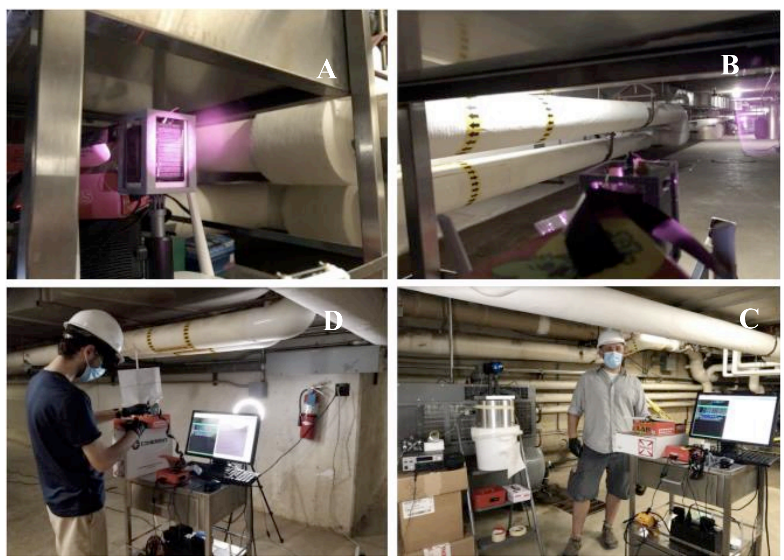


*Figure 18: Power Transfer over 30 Meters. Clockwise from Top Left: (A) The Illuminated FemtoSat Receiving Power, (B) The Optics Tube Transmitting Power Over 30m, (C & D) Configuration of the Experiment.*

The 30m power beaming verification also allowed us to measure the beam's size over that distance. As *Figure 19* shows, the beam width had minimal divergence. This indicates that the useful range of this system could be well over 30 meters with sufficiently accurate pointing actuators. It also illustrates that longer test ranges would be required for such development.

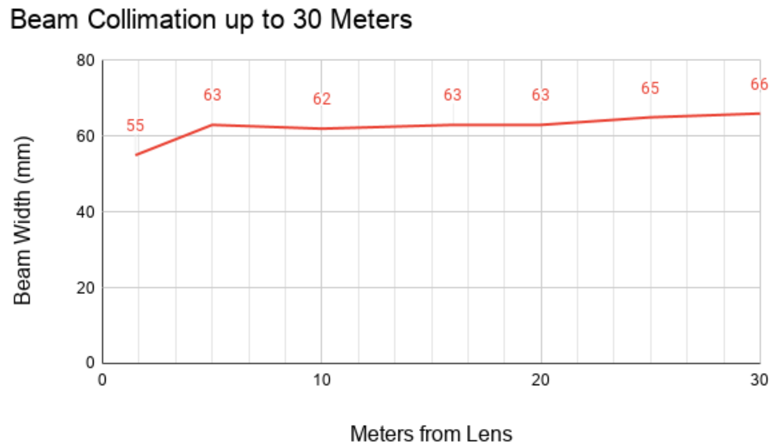


*Figure 19: Collimated Beam Width for a Fixed Focus at Ranges up to 30 Meters. Spot Size Showed Little Divergence.*

**Autonomous Receiver Localization**

The culmination of the receiver detection and aiming system development was a full raster scanning test using the laser at operational power. For this test, the transmitter and FemtoSat were placed within the enclosed vacuum chamber, with windows covered and laser safety interlock engaged. Using power and fiber feedthroughs, the transmitter was fully powered up and receiving signals from the FemtoSat. Upon initialization, the raster scanning process was started, slewing through a 15 degree azimuthal range, increasing elevation 3 degrees per azimuthal sweep. After a few sweeps, the beam fully covered the FemtoSat panels, causing the FemtoSat panel current to spike and signaling the transmitter to stop rotating (also shown in *Figure 9*).

**Lunar Dust**

We performed an initial verification of how much lunar simulants would degrade solar panel performance. LHS-1 and JSC1-A regolith simulants were tested sequentially on the same solar module, cleaning off the prior simulant between tests. The process for applying the lunar simulants involved sprinkling the simulant completely across the panel, then dumping the simulant off the panel to leave a fine layer of dust. This approach simulates how dust would be layered on panels from regolith disturbed from surface movements or vehicle landings. Once dusted with regolith, the panel was mounted at the far end of the optics bench where it was wired into a resistive load. The maximum laser output of 4W was them beamed onto the panel, where the current and voltage were measured. Surprisingly, within the limits of our testing equipment, there was no significant difference in power output between clean panel and dusted panel. Infrared light may

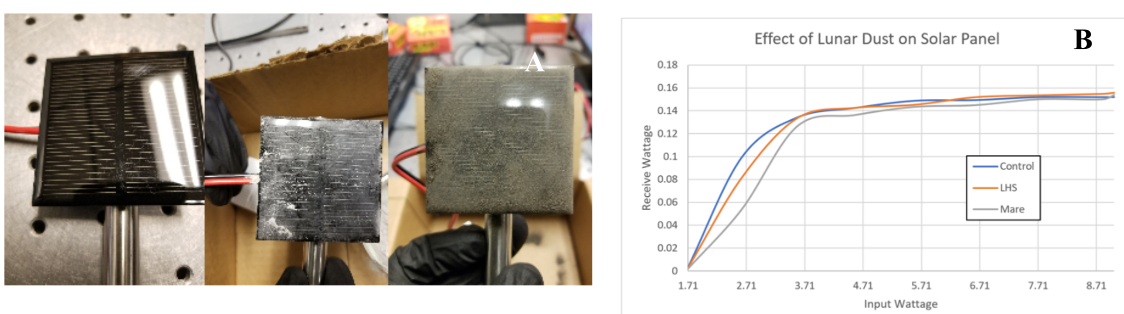


*Figure 20: (A) Control (Left), LHS-1 (Middle), and JSC1-A (Right) Regolith Simulant on Photovoltaic Module. (B): The Effect of Regolith Simulant on Output Power.*

penetrate dust better than shorter wavelengths. *Figure 20* shows the clean versus regolith dusted panels, along with charts showing the power outputs at different laser powers.

Partial panel obstructions were also evaluated, simulating the effect of a FemtoSat panel partially obstructed by regolith. *Figure 21* shows the power output when the panel was partially obstructed, with 1cm and 2cm cell obstructions still outputting power, whereas 2.5cm cell obstruction completely blocked five of the ten cells, preventing power output.

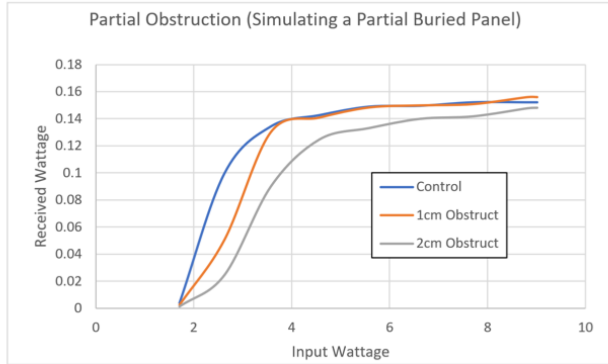


*Figure 21: The Effect of a Partially Buried Receiver Panel on Output Power.*

**Receiver Impact Test**

The receiver impact verification process focused on ensuring the FemtoSat would survive impacting the lunar surface. The CSM Lunar Simulant Testbed was used for this task (*Figure 22*). A mass simulator was 3D printed with the same dimensions and approximately the same mass, allowing the ejection process to be calibrated before testing the actual unit. Two activities were performed, including a vertical drop test and a 45 degree launch test. For the vertical test, the FemtoSat was dropped 2.28m vertically, with a potential energy matching the FemtoSat's parabolic ejection. The launch test ejected the system at 45 degrees from a height of 76cm, achieving a maximum height of 1.15 meters and a distance of 1.96m. These values were selected based on the forces required to achieve the target distance of a 10m deployment on the Moon. The max impact force experienced was 4.35g upon landing in the lunar regolith sandbox. The unit experienced no damage after four successive impact tests, with only a few scuffs on the solar modules. Minimal dust incursion occurred.

*Figure 22: FemtoSat Receiver after Simulated Ejection*

**Vacuum Test**

Environmental testing of the LASER system in the vacuum chamber has yet to be performed due to increasing COVID restrictions. We aim to perform this final verification as able this winter. This verification activity will focus on putting the transmitter and FemtoSat receiver within a cryovac chamber and reducing pressure to 0.1 torr.

## 3.2. Data Collected

**Power beaming over 30 meters**

The end-to-end power efficiency across the 30m gap was 1.56%. While sufficient to meet requirements by charging the battery, the efficiency was limited by the spillage of beam power beyond the panel and choice of resistive load. The beam spillage is fundamental to the design, but our MPPT test showed a better choice of resistive load could increase efficiency to 5.6%.

The beam width results were recorded from images taken of the laser target reticle at different distances along the steam tunnel. We were encouraged to see the minimal beam divergence over the 30m distance, validating our optical design decisions.

**Receiver Localization**
The receiver was found and charged at its max rate of 54mA (Figure 9). The process can be seen at https://youtu.be/suiezE97p18

**Lunar Dust**
Solar panel measurements from regolith simulant obstructions were recorded from multi-meter readings. The minimal impact of regolith on panel output (Figure 20) is an encouraging result, lunar conditions may potentially change the verification conclusion.

**Receiver Impact Test**
Max impact forces experienced by the FemtoSat was 4.35g upon landing in the lunar regolith sandbox. The receiver impact test recorded IMU data at a 2Hz frequency. The IMU data was recorded directly into Excel via the serial output from the receiver ground station. The data, along with physical observations of the FemtoSat unit, are encouraging regarding FemtoSat robustness and survivability.

**Vacuum Test**
The vacuum test will record FemtoSat temperatures, power received, and battery charge state. These values will be recorded by the control interface. It is expected that this test will be performed following the submission of this report.

### 3.3. Challenges
The predominant challenge of the year was and continues to be COVID-19. Lockdowns and global supply chain issues caused schedule delays, and impacted the availability of some components. Schedule disruption cascaded, causing problems with personnel availability and loss of access to laser lab testing facilities sooner than optimal. Procurement, access to the machine shop, vacuum chamber access, and a break in continuity for the receiver team caused schedule slippage. Necessary safety constraints, including safety considerations around a class 4 laser, added complexity.

However, we were able to develop a functional prototype system, and were substantially able to accomplish testing with the exception of the vacuum testing. The resiliency of the team, our flexible and iterative development process, and not least the support and understanding of the BIG Idea Challenge management allowed us to conduct the project successfully in the year of COVID-19.

### 3.4. Testing Facilities
Bench testing and development of the laser subsystem was performed in a dedicated class 4 laser lab at CSM. The FemtoSat receiver was developed and tested under sunlight at UA's SpaceTREx lab. Our 30m power beaming demonstration took place in a steam tunnel underneath CSM's campus, with the supervision and approval of the school's laser safety officer. The receiver impact test took place at the Center for Space Resources' regolith testbed at CSM. Final integration took place at the Center for Space Resources' lab at CSM.

### 3.5. Realistic Simulated Environment
Laser power beaming in atmosphere is a more challenging environment than vacuum, with optical performance expected to be at least as good in vacuum. Receiver impact on the lunar surface was simulated in a realistic regolith environment under atmosphere. Vacuum testing would predict thermal performance in a relevant environment. We did not replicate the lighting environment of the lunar poles, although power

developed by laser illumination was shown to exceed that from solar illumination, indicating that the power beam can be detected against sunlight.

### 3.6. Budget and Schedule Constraints

Our budget was sufficient to cover all development, testing, and contingencies. COVID-19 related disruptions caused schedule slippage, but we were able to develop a complete prototype system and test it at a component and subsystem level in a laboratory environment. Our schedule has not yet accommodated relevant environment testing, which we intend to conduct in the remaining period of performance for the challenge.

## 4. Safety Plan and Protocols Followed

Team safety was of critical importance throughout the project. Key areas of concern included operating a class 4 laser, testing within a cryovac chamber, and utilizing high power CNC and water jet machines. Each of these activities followed approved safety plans.

A laser safety plan was developed by the team based on protocols already developed by CSM and was submitted to BIG Ideas Challenge management at the mid-project review. This plan detailed safe operations of the class 4 laser within both the dedicated laser lab and within a sealed cryovac chamber. Some of the protocols included in this plan include appropriately specified laser safety goggles, laser curtains surrounding the test areas, a buddy system to operate the laser, a dedicated lock-box for keeping the laser driver activation key, and a log book to record all laser firings throughout the experiment. The lab safety officer and our academic supervisor supported the plan, and all appropriate team members took a CSM laser safety training course. No injury to personnel occurred throughout our laser testing.

The Center for Space Resources' lab has established vacuum chamber protocols that were adhered to while testing the system within it. These safety and operational protocols ensured safe operations for both team members and equipment. Examples of protocols include proper chamber preparations and protocols for operating pumps and valves. No damage to personnel or equipment occurred.

The CSM machine shop required adherence to its own safety plan when using its machines. Multiple digital safety courses were undertaken by members who utilized it. These courses covered the use of lathes, mills, the water jet, band saw, belt sander, and 3-axis CNCs. Additionally, in-person training occurred for each machine used. No damage to personnel or equipment occurred throughout the use of the machine shop.

## 5. Path-To-Flight

### 5.1. Lunar Mission

LASER concept development has demonstrated power beaming to small receivers at range up to 30m, with telemetry enabling autonomous localization and closed-loop beam control. Transmitter development showed no major obstacles to flight – testing at the longest ranges available showed good beam quality, which is more challenging in atmosphere than in vacuum. Commodity silicon panels and charge controllers showed satisfactory power conversion efficiency. Further iterations with flight-quality photovoltaics, actuators and computer hardware would move the system towards flight qualification.

The FemtoSat receivers demonstrated the potential for tiny experiments to be useful on the lunar surface. The miniaturization of COTS microcontrollers and batteries offers intriguing performance benefits. Further environmental testing and development of strategies for radiation protection are warranted. Means of emplacing the receivers at greater distances from the lander, such as being emplaced by rovers, could enable their use as localization beacons for navigation within an exploration zone.

The laser transmitter dominates system mass and power – and when used solely to power low mass, low power FemtoSats it undercuts their benefit. A practical path to flight for the laser transmitter should focus on working within a system of systems concept, supporting other remote equipment such as mobile rovers operating in PSRs [Enright]. To do this, further iterations should focus on increasing power and useful range. Receivers optimized for efficient conversion of laser light to power should also be developed, able to intercept more of the beam's energy and efficiently convert it to electricity – particularly for 1060nm light at which efficient, high beam quality lasers emit.

### 5.2. Component Qualification

The next step on the path to flight is to demonstrate our prototype system in the relevant environments. Iterative design would call for system level testing to component failure and addressing the cause of failure in subsequent designs. Replacement of non-flight representative hardware, such as the stepper motors and compute modules, and integration of the laser, power supply, diode driver, and dust shields would increase testing fidelity. Radiation testing could be approached similarly. Our system prototype stands at a medium fidelity, and while designed with flight considerations in mind, none of the components should be considered flight qualified.

### 5.3. Remaining Design Work

The basic feasibility of powering remote receivers with laser beams has been demonstrated. Because a more useful lunar mission would entail higher power and longer range, further design should focus on scaling the system on those axes, along with developing a more efficient receiver. A mission architecture for powering a rover in a PSR, along with an associated ground demonstration, should be developed. With this work done, sufficient risk should be retired for flight hardware development.

### 5.4. Continuation of Concept Development

Our response to NASA's LuSTR solicitation – "Laser Power Beaming for Remote and Mobile Applications" offers a path for continued concept development (*Figure 23* & *Figure* 24) towards a more capable system that would support long-term exploration and utilization of water within PSRs. With a seasoned team from academia, commercial industry, and US government labs, the proposed work offers potential for breakthrough capability with end-to-end efficiency of 10% to 15%, range limited only by pointing accuracy and line-of-sight, and featuring power levels above 100W. Our technical approach will raise the system TRL from 3 to 5 and features an end-to-end ground demonstration over 2km.

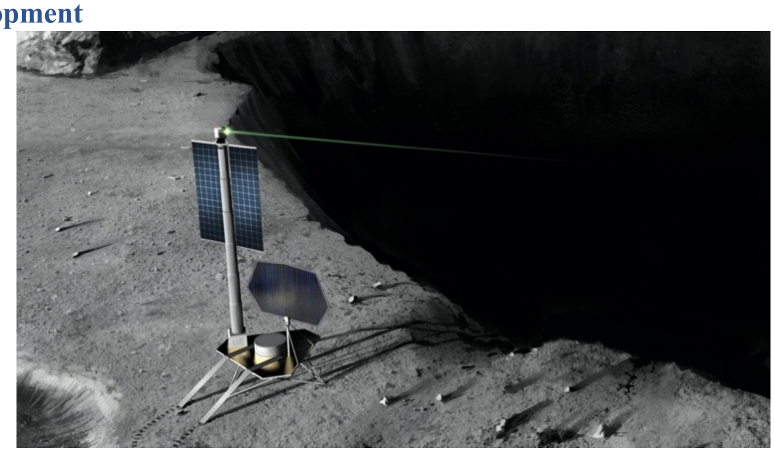

*Figure 23: A Long-Range Laser Power Beaming System with Integrated Power Generation Sending Power to a Prospecting Rover Operating Unseen Deep within a PSR.*

We continue to actively develop laser power beaming technology for lunar surface applications. Enhanced collaboration with commercial partners provides increasing opportunity for developing laser power beaming. We are engaging at an early stage in concept definition for several lunar surface power and mobility systems that could utilize laser power beaming. NASA's Watts on the Moon Challenge provides another opportunity for concept development.

## 6. Results/Conclusions

### 6.1. Achievements of Objectives

We achieved a ground demonstration of laser power beaming, charging a FemtoSat based receiver at 30m range, within a mass and power envelope meeting the challenge requirements if the power draw of non-flight representative actuators is discounted. Autonomous target localization and beam control was demonstrated. Ejection of the receiver from the lander deck was simulated in a regolith testbed, and the receiver was found to survive landing in dusty regolith and impacting a hard surface. Two receivers were produced, as were three iterations of the laser transmitter design.

### 6.2. Key Results

At the outset of this work, the LASER system concept was at TRL 3. We built and demonstrated a prototype system in the laboratory environment, raising the concept to TRL 4. Relevant environment testing can advance the concept to TRL 5/6. We demonstrated laser power beaming, charging the battery of a FemtoSat receiver at a distance of 30m: this establishes a fundamental capability that can be scaled in power and range. Our laser transmitter's optical performance has been validated, and the optics path has been integrated into a functional transmitter. We demonstrated autonomous target localization and beam control. The FemtoSat receiver concept has been validated at TRL 4, and preliminary relevant environment testing has indicated that lunar dust adhesion may have only a minor impact on performance. We anticipate conducting relevant environment testing in vacuum during the reaming period of performance.

### 6.3. Conclusions about Design Solution

With a successful ground demonstration, we have shown that laser power beaming is a feasible way of transmitting energy to remote equipment within line of sight of a lander or power station. The limited power available to auxiliary payloads on first generation CLPS landers is likely to be exceeded by technologies like NASA's proposed 10kW Vertical Surface Array Technology (VSAT). Our optical performance was validated at range up to 30m, and a higher quality laser with harmonic drive actuators should enable ranges limited by line of sight. As a minimum viable demonstration, efficiency of power transmission was not highly optimized, but the system worked as designed and was able to charge the receiver's battery as required.

The laser power beaming demonstration worked well enough that we think our design solution for the challenge, while meeting the requirements, undershoots the potential utility for laser power beaming. A higher power, longer range solution powering a rover operating deep inside a PSR would be a much more valuable application than a minimal proof of concept. A detailed analysis of this opportunity is presented in our LuSTR proposal "Laser Power Beaming for Remote and Mobile Applications".

*Figure 24: A Prospecting Rover Operating Deep within a PSR Powered by a Laser Power Beaming Station Located High Above on the Sunlit Crater Rim.*

We are prepared to scale the LASER concept up and engage commercial partners to create a game-changing capability for exploring deep within PSRs that could be ready by 2025 (*Figure 23 & Figure* 24
*+63*).

## 7. Detailed Timeline

*Table 6: Team LASER's Schedule Over the Period of Performance*

| ID | Task Name | Duration | Start | Finish |
|---|---|---|---|---|
| 1 | Award Notice | 0 | 2/14/20 | 2/14/20 |
| 2 | Develop Actuator Prototype | 35 | 3/2/20 | 4/6/20 |
| 3 | Prototype Actuator Testing | 14 | 4/6/20 | 4/20/20 |
| 4 | Develop Affogato Transmitter | 70 | 4/20/20 | 6/29/20 |
| 5 | Mid-Project Report Deadline | 0 | 5/12/2020 | 5/12/2020 |
| 6 | Pass/Fail Notice | 0 | 5/27/2020 | 5/27/2020 |
| 7 | Second Installment | 14 | 6/1/2020 | 6/15/2020 |
| 8 | Optics Lab Testing | 77 | 6/8/20 | 8/24/20 |
| 9 | Develop Breve Transmitter | 56 | 6/29/20 | 8/24/20 |
| 10 | Breve Transmitter Housing Construction | 21 | 8/24/2020 | 9/14/2020 |
| 11 | Telemetry and RF Localization Integration | 21 | 8/24/2020 | 9/14/2020 |
| 12 | Breve Transmitter Integration | 14 | 9/14/2020 | 9/28/2020 |
| 13 | FemtoSat V2 Construction | 49 | 8/24/2020 | 10/12/2020 |
| 14 | FemtoSat Lunar Simulant Impact Test | 7 | 11/9/2020 | 11/16/2020 |
| 15 | Receiver Deployer Simulation | 35 | 10/19/2020 | 11/23/2020 |
| 16 | Power Efficiency Test (Steam Tunnel) | 14 | 9/14/2020 | 9/28/2020 |
| 17 | Broad Localization Wifi Trans/Beacon Test | 14 | 9/28/2020 | 10/12/20 |
| 18 | Localization and Power Transfer Trans/Rec Test | 14 | 10/12/2020 | 10/26/20 |
| 19 | Technical Paper writing | 33 | 10/26/20 | 11/28/20 |
| 20 | Technical Paper Submission Deadline | 0 | 11/29/2020 | 11/29/20 |
| 21 | Integrated Relevant Environment Testing | 28 | 11/30/20 | 12/28/20 |
| 22 | BIG Idea Challenge Forum | 2 | 1/6/21 | 1/8/21 |

## 8. Detailed Budget

### 8.1. Phase 1 & Phase 2 Funding Awards

*Table 7: Executed Budget*

| **Team LASER Budget Actuals: 11/29/2020** | | | |
|---|---|---|---|
| ***Some payroll liability remains outstanding, additional expenses may be incurred through 01/2021*** | | | |
| **Items** | **Total** | **Phase I (38%)** | **Phase II (62%)** |
| **Salaries/Wages** | | | |
| Faculty Adviser (0.05 FTE, *gratis*) | $0 | $0.00 | $0.00 |
| Graduate Student Labor (@ $25/hr) | $55,383 | $38,720.00 | $16,663.00 |
| **Material/Supplies** | | | |
| Total Materials & Supplies | $21,770 | $1,998.55 | $19,771.93 |
| **Travel Costs** | | | |
| N/A | $0 | $0.00 | $0.00 |
| **Total Expenses** | | | |
| Total Expenses | $77,153 | $40,718.55 | $36,434.93 |
| Awarded Funds | $113,994 | $43,317.72 | $70,676.28 |
| Percent Utilized | 67.7% | 94.0% | 51.6% |

### 8.2. Sponsors and Grants

Our work was entirely supported by the $113,994 BIG Idea Challenge award.

### 8.3. Outside Funding

There was no funding received outside of the BIG Idea challenge award.

### 8.4. Sponsorships or in-kind contributions

Some of our teammates were unable to accept compensation and supported this project with donated time. We also thank our faculty advisors for freely contributed time and advice.

**References**

- Centers, Ross et al., “Development of a Laser Power Beaming Demonstration for CLPS Landers”, International Astronautical Conference 2020
- Centers, Ross, Joshua Schertz, David Dickson, and Phillip Glaser, “Bootstrapping a scalable power infrastructure for lunar mining”, ASCE Earth and Space Conference 2020, Seattle, WA (2020), In press.
- Colaprete, Anthony, et al. "Detection of water in the LCROSS ejecta plume." Science 330.6003 (2010): 463-468.
- “DW1000 Radio IC.” Decawave, www.decawave.com/product/dw1000-radio-ic/. Accessed 20 Nov. 2020.
- Enright, John, and Kieran A. Carroll. "Laser power beaming for lunar polar exploration." 34th Annual International Space Development Conference, Toronto, Canada (2015).
- Kutter, Bernard F., and George F. Sowers. "Cislunar-1000: Transportation supporting a self-sustaining Space Economy." AIAA SPACE 2016. 2016. 5491.
- Landis, Geoffrey A. "Laser Power Beaming for Lunar Polar Exploration." *AIAA Propulsion and Energy 2020 Forum*. 2020.
- Li, Shuai, et al. "Direct evidence of surface exposed water ice in the lunar polar regions." Proceedings of the National Academy of Sciences 115.36 (2018): 8907-8912.
- Puig-Suari, Jordi, Clark Turner, and William Ahlgren. "Development of the standard CubeSat deployer and a CubeSat class PicoSatellite." 2001 IEEE Aerospace Conference Proceedings (Cat. No. 01TH8542). Vol. 1. IEEE, 2001.
- Thangavelautham, Jekanthan, et al. "The SunCube FemtoSat Platform: A Pathway to Low-Cost Interplanetary Exploration." 6th Interplanetary CubeSat Workshop, Oxford, England. 2016
- “TinyDuino Overview.” TinyCircuits, tinycircuits.com/pages/tinyduino-overview. Accessed 20 Nov. 2020.
- Yavari, Mohammadreza, and Bradford Nickerson. Ultra Wideband Wireless Positioning Systems. 2014. https://www.decawave.com/wp-content/uploads/2018/12/Ultra-Wideband-Wireless-Positioning-Systems_2014-03-27.pdf